Electrochimica Acta 55 (2010) 8595–8599

Contents lists available at ScienceDirect

Electrochimica Acta

journal homepage: www.elsevier.com/locate/electacta

High performance $Li_3V_2(PO_4)_3$/C composite cathode material for lithium ion batteries studied in pilot scale test

Zhenyu Chen [a], Changsong Dai [a,*], Gang Wu [b], Mark Nelson [b], Xinguo Hu [a], Ruoxin Zhang [c], Jiansheng Liu [c], Jicai Xia [c]

[a] School of Chemical Engineering and Technology, Harbin Institute of Technology, Harbin 150001, China
[b] Materials Physics and Applications Division, Los Alamos National Laboratory, Los Alamos, NM 87545, USA
[c] Battery Material Business Division, Guangzhou Tinci Materials Technology Co., Ltd., Guangzhou 510760, China

ARTICLE INFO

Article history:
Received 11 March 2010
Received in revised form 19 July 2010
Accepted 24 July 2010
Available online 3 August 2010

Keywords:
Lithium ion battery
Cathode materials
Lithium vanadium phosphate
High-rate performance
Carbothermal reduction method

ABSTRACT

$Li_3V_2(PO_4)_3$/C composite cathode material was synthesized via carbothermal reduction process in a pilot scale production test using battery grade raw materials with the aim of studying the feasibility for their practical applications. XRD, FT-IR, XPS, CV, EIS and battery charge–discharge tests were used to characterize the as-prepared material. The XRD and FT-IR data suggested that the as-prepared $Li_3V_2(PO_4)_3$/C material exhibits an orderly monoclinic structure based on the connectivity of PO_4 tetrahedra and VO_6 octahedra. Half cell tests indicated that an excellent high-rate cyclic performance was achieved on the $Li_3V_2(PO_4)_3$/C cathodes in the voltage range of 3.0–4.3 V, retaining a capacity of 95% (96 mAh/g) after 100 cycles at 20*C* discharge rate. The low-temperature performance of the cathode was further evaluated, showing 0.5*C* discharge capacity of 122 and 119 mAh/g at −25 and −40 °C, respectively. The discharge capacity of graphite//$Li_3V_2(PO_4)_3$ batteries with a designed battery capacity of 14 Ah is as high as 109 mAh/g with a capacity retention of 92% after 224 cycles at 2*C* discharge rates. The promising high-rate and low-temperature performance observed in this work suggests that $Li_3V_2(PO_4)_3$/C is a very strong candidate to be a cathode in a next-generation Li-ion battery for electric vehicle applications.

1. Introduction

The high stored energy density, both volumetric and gravimetric, of Li-ion batteries have resulted in their successful commercialization in portable electronic device applications such as cellular phones and lap-top computers for a long time. However, cost, safety, energy density, rate capability, and service life issues remain big challenges plaguing the development of the Li-ion batteries for the potential mass market of electric vehicles (EV) and hybrid electric vehicles (HEV) [1–3]. And one bottle neck for the application of lithium ion batteries is cathode materials. Recently, polyanion-based materials $(PO_4)^{y-}$ have emerged as the most promising cathode candidates, due to their high redox potentials and energy density, and excellent thermal and electrochemical stability. In this family, the advantages in using Fe-based compounds are the abundance, low cost, and stability against over-charge/discharge, whereas lithium iron phosphate ($LiFePO_4$) cathodes have been found to be limited by their low electron conductivity and low Li-ion diffusion rates, resulting in poor rate capacity and low-temperature performance. Some recent research indicates that there might be some ways to overcome this limitation by doping with carbon and other metals (Al, Cu, Mg, V, etc.) [4]. $Li_3V_2(PO_4)_3$ exhibits different characteristics from $LiFePO_4$ and seems a viable alternative. Its theoretical capacity utilizing all of three Li^+ ions in a voltage range of 3.0–4.8 V is 197 mAh/g, which is the highest in all phosphate cathode materials [5–7]. Unlike the one-dimensional channels in LiFePO4, the three-dimensional framework in $Li_3V_2(PO_4)_3$ that contains larger polyanion and interconnected interstitial space is favorable to stabilize the structure and results in a high Li^+ ion diffusion coefficient [8]. These unique structural characteristics suggest that $Li_3V_2(PO_4)_3$ cathode should possess excellent high-rate performance and cyclic stability [7,9,10]. Like other phosphates, $Li_3V_2(PO_4)_3$ also is a safe cathode material [9]. These advantages make it an ideal cathode material for next-generation lithium ion batteries, especially for EV and HEV applications. The carbothermal reduction (CTR) method first developed by Huang and Saidi [7,11] has proven to be a particularly efficient and economical way to synthesize $Li_3V_2(PO_4)_3$ composite cathode materials, in which the reduction of V^{3+} and carbon coating can be realized in a single step. This method also has been considered to be the most promising in industrial production applications.

* Corresponding author.
Tel.: +86 451 86413751; fax: +86 451 86413721/86221048.
E-mail address: changsd@hit.edu.cn (C. Dai).

0013-4686/$ – see front matter © 2010 Elsevier Ltd. All rights reserved.
doi:10.1016/j.electacta.2010.07.068

Previous research on $Li_3V_2(PO_4)_3$ cathode material was focused on doping of carbon coating [12,13] and metal ions [14–18] to improve their electrochemical performance. However, most studies were carried out on small experimental scale. Little pilot testing for practical application such as automotive power has been reported. In this work, with the aim of studying the feasibility of practical applications, the CTR method was further developed to synthesize $Li_3V_2(PO_4)_3$/C composite cathodes in a pilot test with a yield capacity of 5.0 kg per batch using battery grade raw materials. Diverse battery tests were performed to systematically study high-rate and low-temperature discharge cyclic performance using Li//$Li_3V_2(PO_4)_3$ coin cell and actual graphite//$Li_3V_2(PO_4)_3$ complete cells with a designed capacity of 14 Ah.

2. Experimental

2.1. Cathode synthesis

$Li_3V_2(PO_4)_3$/C composite powders were synthesized using battery grade $LiOH{\cdot}H_2O$, V_2O_5 and $NH_4H_2PO_4$ at stoichiometric ratios via a carbothermal reduction process with sucrose as the carbon source. The ball milled mixture was first heated to 300–350 °C under an argon atmosphere in order to remove NH_3, H_2O, etc., and then heat treated in a pilot-test atmosphere converter (Hotblue, China) at a temperature of 800–850 °C in an argon atmosphere for 16–24 h to generate the $Li_3V_2(PO_4)_3$/C composite materials.

2.2. Physical and electrochemical characterization

The crystal structure of the as-prepared $Li_3V_2(PO_4)_3$/C was characterized by X-ray diffraction (XRD) using a D/max-γβ X-ray diffractometer (Rigaku, Japan) with Cu Kα radiation. Fourier transform infrared (FT-IR) absorption spectra were recorded by an Avatar360 Fourier transform infrared spectrometer (Nicolet, America). X-ray photoelectron spectroscopy (XPS) was performed with a PHI5700 type analyzer (Electrophysics, America) to evaluate the oxidation states of elements in $Li_3V_2(PO_4)_3$/C samples. The cathode particle size was measured using an LS900 laser particle size analyzer (Malvern, England). Also, the carbon content in the composite cathode was determined using a TOC-VCPN-(SSM-5000A) type carbon–sulfur analyzer (Shimadzu, Japan).

The cathode slurry was prepared by mixing as-synthesized $Li_3V_2(PO_4)_3$/C powders with acetylene black and polyvinylidene difluoride (PVDF) with a mass ratio of 80:10:10 in *n*-methyl-2 pyrrolidone (NMP) solvent. Subsequently, this mixture was coated on an aluminum current collector. The separator was a Celgard 2400, and the electrolyte was 1 M $LiPF_6$ in a blended ethylene carbonate (EC), dimethyl carbonate (DMC) and diethylene carbonate (DEC) with a volume ratio of 1:1:1. CR2025 coin cells were assembled in a glove box filled with high purity argon. The coin cells were galvanostatically charged and discharged at different rates and temperatures using a multi-channel battery test system (Neware, China). Cyclic voltammetry (CV) was carried out on a CHI-630b electrochemical workstation (Chenhua, China). The EG&G PARC M 273 and M398 software packages were used for electrochemical impedance spectroscopy (EIS) with a frequency range from 10 K to 0.1 Hz. The EIS data were further interpreted on the basis of equivalent electrical circuits using fitting software (EQUIVCRT).

3. Results and discussion

3.1. Physical characterization of $Li_3V_2(PO_4)_3$/C

Fig. 1 shows the XRD pattern of the as-synthesized $Li_3V_2(PO_4)_3$/C sample. All diffraction peaks could be indexed well to monoclinic $Li_3V_2(PO_4)_3$/C structure with the space group of $P2_1/n$. The cell parameters were determined as follows: $a = 0.86697$ nm, $b = 0.85959$ nm, $c = 1.20464$ nm, $\beta = 90.23°$, and cell volume = 0.89774 nm^3, which is very close to the data in previous reports synthesized from small-scale experiments [16,19,20]. As shown in Fig. 2, FT-IR spectroscopy of the sample was recorded to determine the nature of bonds in the $Li_3V_2(PO_4)_3$/C material. The bands at 501, 635 and 968 cm^{-1} can be assigned to the vibration of bonds between V^{3+} and O^{2-} in the isolated VO_6 octahedra. The bands at 950 and 760 cm^{-1} which are characteristic of the presence of V^{5+} ions in isolated VO_6 octahedra were not observed, indicating that the V^{5+} ions have been reduced to V^{3+}. The bands at 575 and 1048 cm^{-1} suggest the presence of P–O bonds of PO_4 tetrahedra. The infrared bands in the range of 1150–1250 cm^{-1} can be attributed to the stretching vibrations of terminal PO_4 units. Combination of XRD and FT-IR results suggest that the as-prepared $Li_3V_2(PO_4)_3$/C material exhibit an orderly monoclinic structure based on the connectivity of PO_4 tetrahedra and VO_6 octahedra.

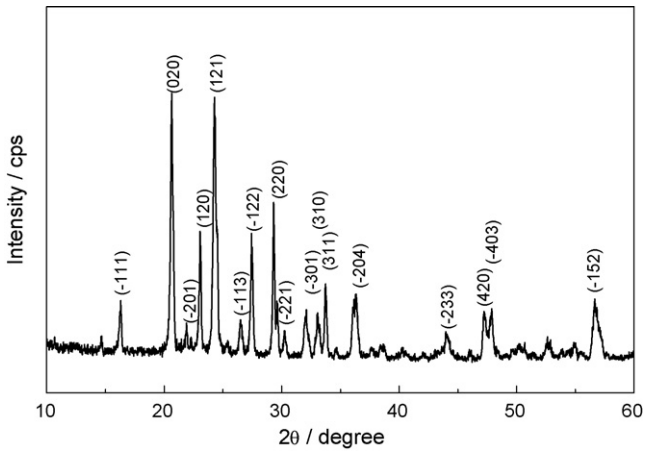

Fig. 1. XRD pattern of as-prepared $Li_3V_2(PO_4)_3$/C materials.

The oxidation states of the elements in $Li_3V_2(PO_4)_3$/C were further studied by XPS as shown in Fig. 3a. Generally, a lithium peak should be found at a binding energy around 60 eV, but it cannot be clearly detected here. The possible reason is that the sensitivity of the equipment is not high enough to detect this lithium peak. Other elements in $Li_3V_2(PO_4)_3$/C were confirmed using XPS analysis. Fig. 3b shows the V 2p XPS core levels for $Li_3V_2(PO_4)_3$/C materials. A dominant single peak at a binding energy of 517.2 eV can be attributable to the oxidation state of V^{3+}, in a good agreement with Ren's report [16]. Above characterization strongly suggested

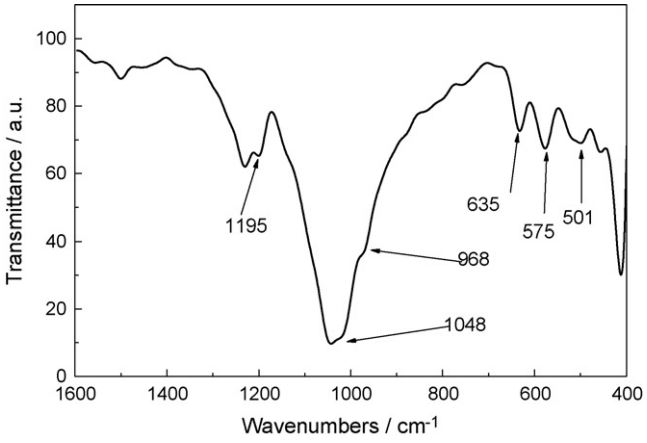

Fig. 2. FT-IR spectrum of as-prepared $Li_3V_2(PO_4)_3$/C cathode materials.

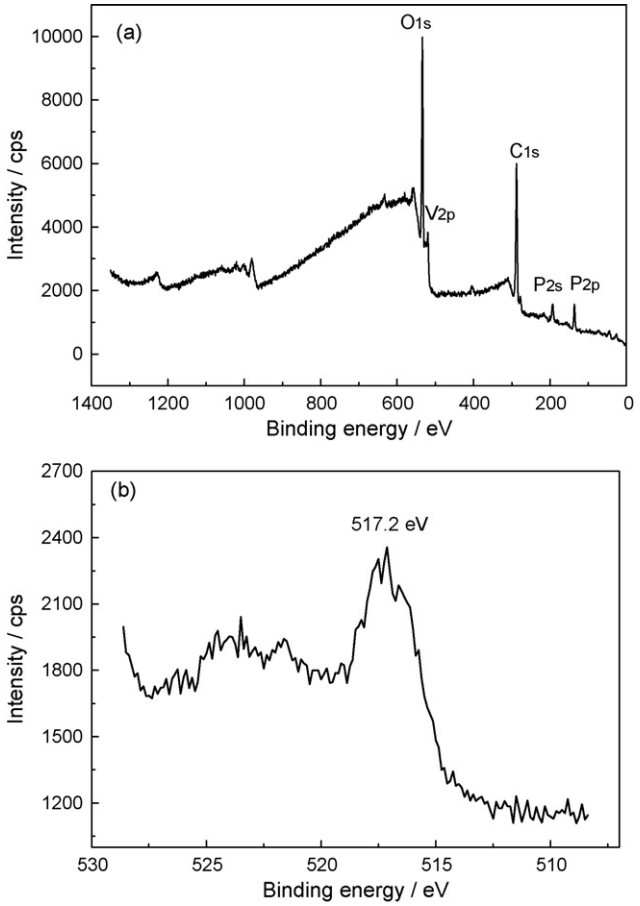

Fig. 3. (a) XPS spectra of as-prepared $Li_3V_2(PO_4)_3$/C materials and (b) XPS core level of V 2p.

that the $Li_3V_2(PO_4)_3$/C material prepared using the pilot-test atmosphere converter have the same structure and characteristic as those prepared on small experimental scales in previous work [16,19,20].

Particle size and carbon content are important properties for $Li_3V_2(PO_4)_3$/C composite cathode materials, which greatly affect cathode performance. In this work, using a laser particle size analyzer, the D_{50} value of the as-prepared $Li_3V_2(PO_4)_3$/C material was determined to be around 7.52 μm. Meanwhile, the carbon content of the sample was optimized to be around 3.4 wt% using a carbon–sulfur analyzer.

3.2. Li^+ insertion/desertion behavior of $Li_3V_2(PO_4)_3$/C

A cyclic voltammogram of $Li_3V_2(PO_4)_3$/C obtained at a scan rate of 0.05 mV/s is shown in Fig. 4. Three anodic and three cathodic peaks were detected during the anodic and cathodic scans in given potential windows (3.0–4.3 V), respectively. Three peaks (3.65, 3.70 and 4.12 V) appear in the anodic scan corresponding to a sequence of phase transition processes accompanying the Li^+ extraction at different stages from $Li_xV_2(PO_4)_3$ (x = 3.0, 2.5, 2.0 and 1.0). On the other hand, in the cathodic scan, three observed peaks (3.54, 3.63 and 4.01 V) are associated with a sequence of phase transition processes related to Li^+ insertion at different phases described above [6]. Generally, the potential interval between the anodic peak and the cathodic peak is an important parameter for evaluation of the reversibility of an electrochemical reaction. The potential differences between oxidation peaks and reduction peaks are 0.11, 0.07 and 0.11 V for the three redox couples, respectively. These small

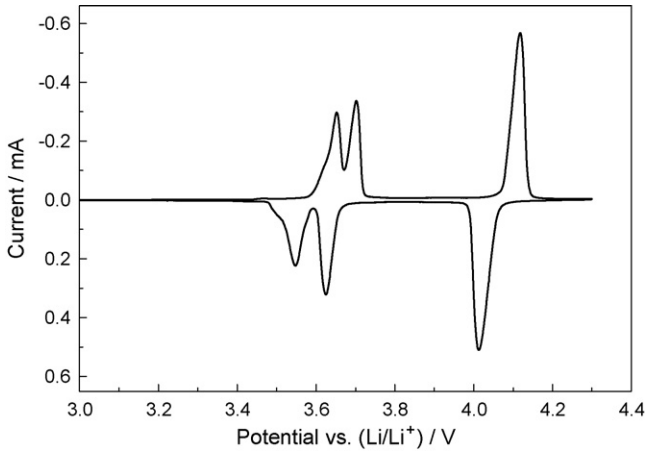

Fig. 4. CV curve of $Li_3V_2(PO_4)_3$/C cathode at a scan rate of 0.05 mV/s between 3.0 and 4.8 V vs Li/Li^+.

potential differences observed in the CV suggests a good reversibility for Li extraction/insertion in $Li_3V_2(PO_4)_3$ cathode.

In this work, EIS was further used to investigate the electrochemical kinetics of $Li_3V_2(PO_4)_3$/C when it was charged to different voltages. The Nyquist plots are compared in Fig. 5a and the equivalent circuit used to fit the data is shown in Fig. 5b. The fitted parameters are summarized in Fig. 6. In Fig. 5b, R_u designates the electronic conductivity of the $Li_3V_2(PO_4)_3$/C sample; R_S and C_S are the resistance and capacitance of solid electrolyte interface (SEI) films; the constant phase element Q is associated with the capacitance of the double layer; R_{ct} designates the charge transfer resistance when Li^+ ions extract from $Li_3V_2(PO_4)_3$ cathode; Z_w is the solid phase diffusion resistance of Li^+. As shown in Fig. 6, the R_{ct} and Z_w are found to be decreasing with charging voltage up to 4.3 V, indication of increases of electrochemical reactivity and ionic conductivity during the first two Li^+ extraction processes.

In order to learn more about structural changes of $Li_3V_2(PO_4)_3$ during the electrochemical cycle process, XRD was employed to study the $Li_3V_2(PO_4)_3$/C samples after 4 and 100 cycles in a voltage

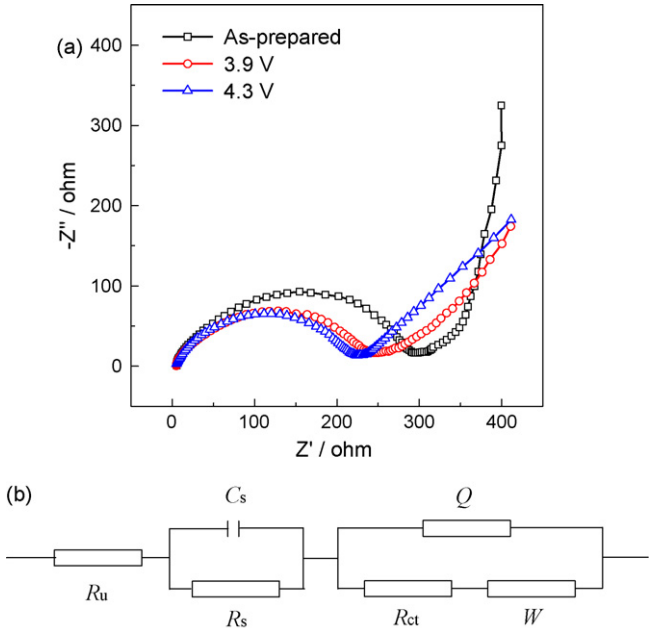

Fig. 5. (a) Nyquist plots of $Li_3V_2(PO_4)_3$ charging to different voltages and (b) equivalent circuit for fitting EIS data.

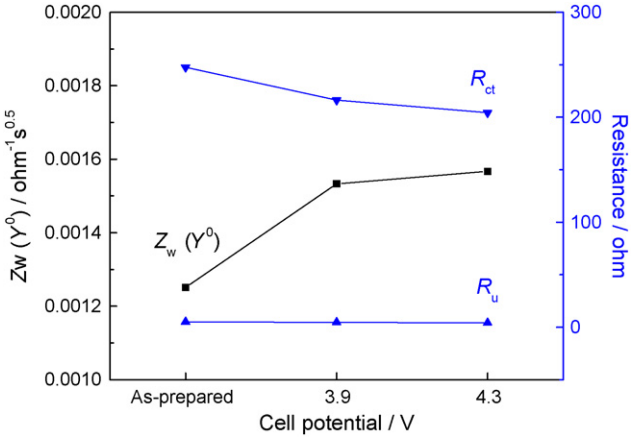

Fig. 6. R_u, R_{ct} and $Z_w(Y^0)$ values in EIS as a function of voltage in Li//$Li_3V_2(PO_4)_3$/C cells.

range of 3.0–4.3 V, as shown in Fig. 7. No obvious structural change was observed from the XRD patterns during cycling, presenting a similar order monoclinic structure. This comparison implies a structural stability of $Li_3V_2(PO_4)_3$/C material is maintained cycling in the investigated voltage range.

3.3. Charge–discharge performance of $Li_3V_2(PO_4)_3$/C cathode

Cyclic performance for the $Li_3V_2(PO_4)_3$/C cathode material was further evaluated in the range of 3.0–4.3 V at different charge/discharge rates as shown in Fig. 8. Operating at 1*C* charge and 10*C* discharge rates, discharge specific capacity of the $Li_3V_2(PO_4)_3$/C cathode material was 113 mAh/g with capacity retention of 98% after 100 cycles. At 10*C* charge and discharge rates, very similar discharge capacities were measured for the 2nd and 100th cycles, around 106 and 105 mAh/g, respectively. It is worth noting that, in the case of 1*C* charge and 20*C* discharge rates, the

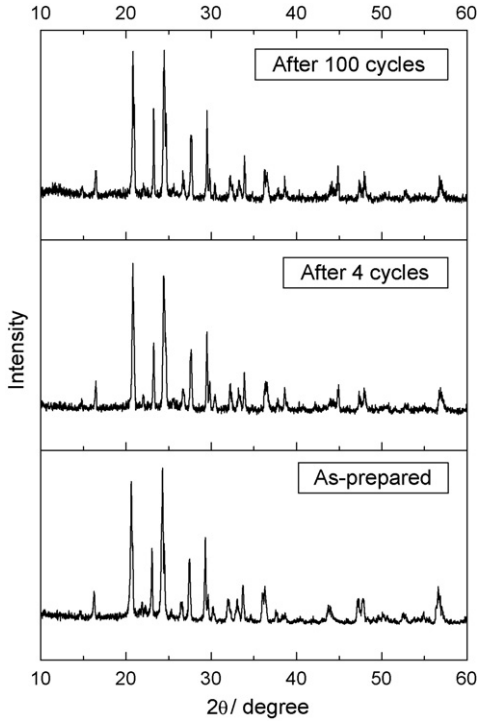

Fig. 7. The XRD patterns of (a) as-prepared $Li_3V_2(PO_4)_3$, (b) $Li_3V_2(PO_4)_3$ after 4 cycles in 3.0–4.3 V and (c) $Li_3V_2(PO_4)_3$ after 100 cycles in 3.0–4.3 V.

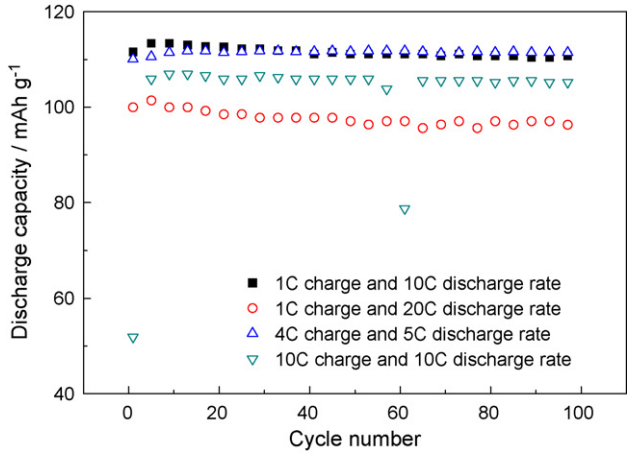

Fig. 8. Cyclic performance of $Li_3V_2(PO_4)_3$/C cathode at various charge and discharge rates.

discharge capacities of the 3rd and 100th cycles still are able to remain 101 and 96 mAh/g, respectively, with a capacity retention of 95%. The excellent high-rate cyclic performance observed with the synthesized $Li_3V_2(PO_4)_3$/C composite cathode is of importance to automotive applications. When compared with $Li_3V_2(PO_4)_3$/C samples prepared in a tube furnace on laboratory scale [8,12,17,21–23], the cathode materials synthesized in the pilot scale atmosphere converter have better charge–discharge rate performance.

To further study the feasibility of $Li_3V_2(PO_4)_3$/C cathode in practical applications, its cyclic performance at low temperatures was studied. The cell was charged to 4.3 V with 0.5*C* rate at 25 °C, then the discharging capacities were recorded at −25 or −40 °C using the same rate. As shown in Fig. 9, it can be seen that although the cell potential decreased at the lower temperature, the difference in discharge capacity with temperature is insignificant. When discharging at −25 °C, the initial and 10th cycle discharge capacities of $Li_3V_2(PO_4)_3$/C were measured to be 120 and 122 mAh/g, respectively, very similar to the discharge capacity at 25 °C (122 mAh/g). When discharging to 3.0 and 2.5 V at −40 °C, the capacities are able to remain at 110 and 119 mAh/g, respectively. These results indicate that the $Li_3V_2(PO_4)_3$/C cathode synthesized in the pilot test exhibits a good low-temperature discharging performance and cyclic stability.

The charge–discharge cyclic performance of the $Li_3V_2(PO_4)_3$/C cathode was further evaluated in a complete lithium ion battery using a graphite anode with a designed battery capacity of

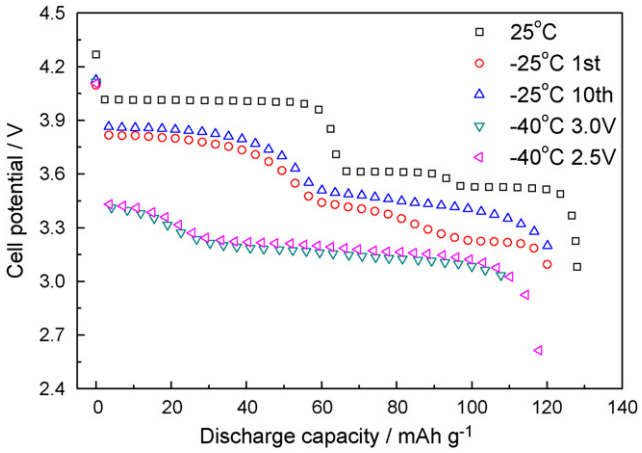

Fig. 9. Discharge curves of $Li_3V_2(PO_4)_3$/C cathode at low temperature.

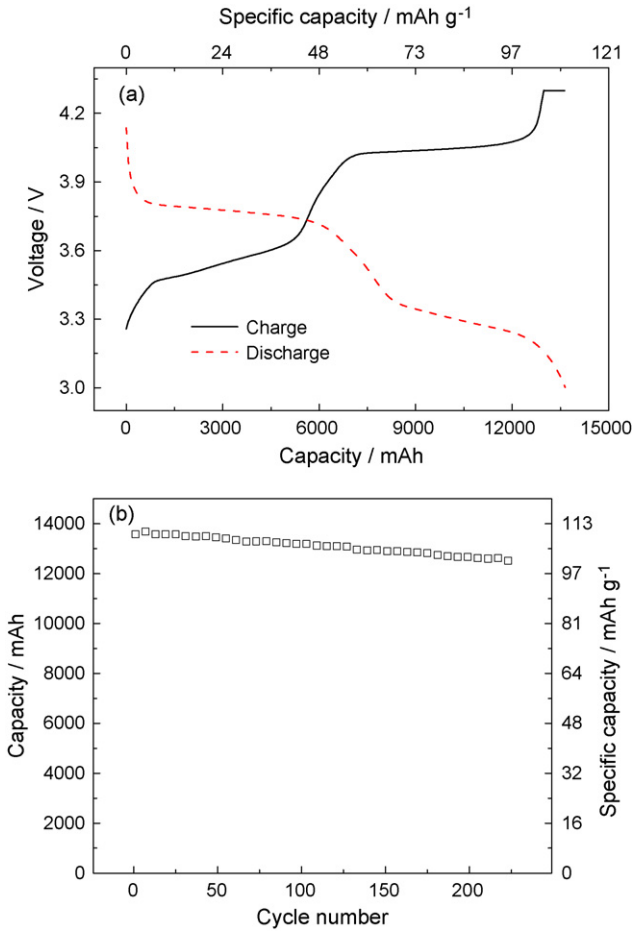

Fig. 10. Initial charge–discharge curves (a) and cycle performance (b) of a fabricated lithium ion battery with a designed capacity of 14 Ah using a graphite anode and a $Li_3V_2(PO_4)_3$/C composite cathode.

14 Ah. Using 1*C* charge and 2*C* discharge rates, the capacity of the $Li_3V_2(PO_4)_3$/C composite cathode was 109 mAh/g (Fig. 10a). Importantly, the capacity retention was 92% after 224 cycles (Fig. 10b).

4. Conclusions

$Li_3V_2(PO_4)_3$/C composite cathode material with outstanding high-rate and low-temperature discharge performance was successfully synthesized through carbothermal reduction method in a pilot scale test. In a voltage range of 3.0–4.3 V, after charging at 1*C* rate, the discharging capacity retentions at 10*C* and 20*C* rates for the $Li_3V_2(PO_4)_3$/C cathode can be as high as 98% (105 mAh/g) and 95% (96 mAh/g) after 100 cycles, respectively. Also, the $Li_3V_2(PO_4)_3$/C cathode demonstrated a good low-temperature cycle performance with a discharge capacity of 122 mAh/g at −25 °C, and 119 mAh/g at −40 °C. The study of a complete Li-ion battery with a designed battery capacity of 14 Ah further verified that it is very feasible to develop $Li_3V_2(PO_4)_3$/C composite cathode material for practical applications in lithium ion batteries, showing a discharging capacity of 109 mAh/g with a capacity retention of 92% after 224 cycles at 1*C* charge and 2*C* discharge rates. This encouraging high-rate and low-temperature performance as well as the actual battery cyclic stability observed in this work suggest that $Li_3V_2(PO_4)_3$/C holds great promise to be a cathode in a next-generation Li-ion battery for electric vehicle applications.

Acknowledgements

The authors acknowledge the financial support for this work from Post-Doctoral Science and Research Startup Fund of Heilongjiang Province, and Scientific and Technological Project of Huangpu, Guangzhou (No. 0950).

References

[1] J.B. Goodenough, Y. Kim, Chem. Mater. 22 (2010) 587.
[2] D. Jugovic, D. Uskokovic, J. Power Sources 190 (2009) 538.
[3] B.J. Landi, M.J. Ganter, C.D. Cress, R.A. Dileo, R.P. Raffaelle, Energy Environ. Sci. 2 (2009) 638.
[4] M.R. Yang, W.H. Ke, S.H. Wu, J. Power Sources 165 (2007) 646.
[5] S.C. Yin, H. Grondey, P. Strobel, M. Anne, L.F. Nazar, J. Am. Chem. Soc. 125 (2003) 10402.
[6] H. Huang, S.C. Yin, T. Kerr, N. Taylor, L.F. Nazar, Adv. Mater. 14 (2002) 1525.
[7] H. Huang, T. Faulkner, J. Barker, M.Y. Saidi, J. Power Sources 189 (2009) 748.
[8] A.P. Tang, X.Y. Wang, G.R. Xu, Mater. Lett. 63 (2009) 1439.
[9] J. Barker, M.Y. Saidi, J.L. Swoyer, Electrochem. Solid State Lett. 6 (2003) A53.
[10] X.H. Rui, C. Li, C.H. Chen, Electrochim. Acta 54 (2009) 3374.
[11] M.Y. Saidi, J. Barker, H. Huang, J.L. Swoyer, G. Adamson, J. Power Sources 119–121 (2003) 266.
[12] M.M. Ren, Z. Zhou, X.P. Gao, W.X. Peng, J.P. Wei, J. Phys. Chem. C 112 (2008) 5689.
[13] X.C. Zhou, Y.M. Liu, Y.H. Guo, Electrochim. Acta 54 (2009) 2253.
[14] M. Sato, H. Ohkawa, K. Yoshida, M. Saito, K. Uematsu, K. Toda, Solid State Ionics 135 (2000) 137.
[15] D. Morgan, G. Ceder, M.Y. Saidi, J. Barker, J. Swoyer, H. Huang, G. Adamson, J. Power Sources 119–121 (2003) 755.
[16] M.M. Ren, Z. Zhou, Y.Z. Li, X.P. Gao, J. Yan, J. Power Sources 162 (2006) 1357.
[17] Y.H. Chen, Y.M. Zhao, X.N. An, J.M. Liu, Y.Z. Dong, L. Chen, Electrochim. Acta 54 (2009) 5844.
[18] Q. Kuang, Y.M. Zhao, X.N. An, J.M. Liu, Y.Z. Dong, L. Chen, Electrochim. Acta, doi:10.1016/j.electacta.2009.10.028.
[19] P. Fu, Y. Zhao, X. An, Y. Dong, X. Hou, Electrochim. Acta 52 (2007) 5281.
[20] Y.Z. Li, Z. Zhou, M.M. Ren, X.P. Gao, J. Yan, Electrochim. Acta 51 (2006) 6498.
[21] P. Fu, Y.M. Zhao, Y.Z. Dong, X.N. An, G.P. Shen, Electrochim. Acta 52 (2006) 1003.
[22] X.C. Zhou, Y.M. Liu, Y.L. Guo, Solid State Commun. 146 (2008) 261.
[23] L.J. Wang, X.C. Zhou, Y.L. Guo, J Power Sources 195 (2010) 2844.